ISSN 0965-5425, Computational Mathematics and Mathematical Physics, 2013, Vol. 53, No. 10, pp. 1499–1511. © Pleiades Publishing, Ltd., 2013.
Original Russian Text © E.N. Aristova, S.V. Martynenko, 2013, published in Zhurnal Vychislitel'noi Matematiki i Matematicheskoi Fiziki, 2013, Vol. 53, No. 10, pp. 1684–1697.

Bicompact Rogov Schemes for the Multidimensional Inhomogeneous Linear Transport Equation at Large Optical Depths

E. N. Aristova[a, b] and S. V. Martynenko[b]

[a] *Keldysh Institute of Applied Mathematics, Russian Academy of Sciences, Miusskaya pl. 4, Moscow, 125047 Russia*
[b] *Moscow Institute of Physics and Technology, Institutskii per. 9, Dolgoprudnyi, Moscow oblast, 141700 Russia*
e-mail: aristova@imamod.ru

Received March 22, 2013

Abstract—Bicompact Rogov schemes intended for the numerical solution of the inhomogeneous transport equation are extended to the multidimensional case. A factorized modification of the method without using splitting in directions or introducing additional half-integer spatial points is proposed. As its original counterpart, the scheme is fourth-order accurate in space and third-order accurate in time. In the case of one dimension, a higher order accurate scheme on a minimal stencil is constructed using the node values of the unknown function and, in addition, its integral averages over a spatial cell. In the case of two dimensions, the set of unknowns in a given cell is expanded to four. The resulting system of equations is solved for the expanded set of variables by the running calculation method, which reflects the characteristic properties of the transport equation without explicit use of characteristics. In the case of large optical depths and a piecewise differentiable solution, a monotonization procedure is proposed based on the Rosenbrock scheme with complex coefficients.

DOI: 10.1134/S0965542513090042

Keywords: transport equation, bicompact schemes, Runge–Kutta methods, Rosenbrock scheme with complex coefficients.

1. INTRODUCTION

Neutron transport or unpolarized radiation transfer is described by a simple partial differential equation, namely, by the linear inhomogeneous transport equation. Numerous methods are available for the numerical solution of equations of this type. An important place among them is occupied by methods that make use of the characteristic properties of the transport equation. However, the direct application of characteristics in the numerical solution is not always convenient. In [1–6] Rogov proposed a method for solving the homogeneous transport equation that combines a minimal two-point stencil in each direction, a high-order accurate approximation (fourth in space and third in time), and monotonicity, which is achieved by hybridizing solutions produced by third- and first-order accurate schemes. The resulting system of equations can be solved using the running calculation method, which reflects the characteristic properties of the transport equation without explicit use of characteristics. Another beneficial property of bicompact schemes is that all their properties are preserved in the case of strongly heterogeneous meshes. In [7, 8] this method was developed as applied to hyperbolic systems of equations, including gas dynamics equations. However, its application to the inhomogeneous transport equation [9] required the introduction of a somewhat different monotonization procedure in the case of large optical depths (see [10]).

Now Shil'kov is developing the method of Lebesgue averaging of absorption coefficients (see [11–24]). In computational complexity, this method is comparable to the multigroup approximation, while its numerical accuracy is similar to that of the line-by-line methods (see [21–24]). The transition to Lebesgue coefficients means that the range of absorption coefficients becomes much wider than in the multigroup approach, and it is extended primarily toward larger optical depths. In atmospheric radiation problems, for example, this means that the atmospheric optical depths for photons of different energy vary by ten and more orders of magnitude in the transition from the centers of lines to the edges. This wide range of coefficients cannot be balanced by reasonable spatial mesh refinement so that the optical depth of cells is less than or on the order of unity for all energies. The *optical depth* is a dimensionless quantity equal to the product of the absorption coefficient σ [cm^{-1}] and the characteristic cell size h [cm]. Thus, in the case

of cells with a large optical depth, the correct reproduction of the behavior of the numerical solution becomes the basic requirement for a difference scheme applied to the linear transport equation.

2. BICOMPACT ROGOV SCHEMES FOR THE INHOMOGENEOUS TRANSPORT EQUATION CONSTRUCTED BY THE METHOD OF LINES

The linear inhomogeneous nonstationary particle transport equation has the form

$$\frac{\partial u}{\partial t} + a\frac{\partial u}{\partial x} + b\frac{\partial u}{\partial y} + \sigma u = Q. \tag{1}$$

In plane-parallel geometry, the coefficients a and b are interpreted as the projections of the particle direction onto the coordinate axes, σ is the absorption coefficient, and Q is the source. Note, however, that Eq. (1) can be treated as a reduced (divided by the direction projection onto the z axis) stationary transport equation in three-dimensional geometry if the time derivative is replaced by the derivative with respect to the third spatial variable.

For the initial–boundary value problem to be well posed, we need to set conditions on the boundaries of the computational domain. Depending on the signs of a and b, a boundary value problem is posed on those boundaries where a characteristic enters the computational domain. Assuming that both these constants are positive, we supplement Eq. (1) with boundary conditions of the form

$$\begin{aligned} u(x,y,0) &= f(x,y), \quad 0 \le x \le X, \quad 0 \le y \le Y; \\ u(0,y,t) &= p(y,t), \quad 0 \le y \le Y, \quad 0 \le t \le T; \\ u(x,0,t) &= q(x,t), \quad 0 \le x \le X, \quad 0 \le t \le T. \end{aligned} \tag{2}$$

The other combinations of the signs of a and b are treated straightforwardly.

The idea underlying bicompact schemes in the case of one dimension is twofold: (i) the method of lines is applied in such a manner that a difference approximation is used for some of the variables, while some of the terms in the equation are left in differential form; and (ii) the set of unknowns is increased. Initially, a primitive of the unknown function was used as a second unknown and the difference scheme was written for the difference between primitives in two neighboring nodes. However, the scheme became more convenient and clearer when the additional unknown was specified as an integral average over a cell. The integral averages are related to the nodal values of the function and its derivative by the Euler–Maclaurin formula

$$\int_{x_l}^{x_{l+1}} u\,dx = \frac{h_{l+1}}{2}(u_{l+1} + u_l) - \frac{h_{l+1}^2}{12}(u_{x,l+1} - u_{x,l}) + O(h_{l+1}^4). \tag{3}$$

By using (3), we obtain a system of two dynamic equations, of which one is an exact consequence of the original transport equation, while the other is derived to fourth-order accuracy in space (see [3, 10]). A time approximation can be obtained using various schemes, for example, third-order accurate diagonal implicit Runge–Kutta methods.

In the multidimensional case, Rogov used either splitting in directions [5] or a scheme with half-integer nodes [8] and computed integral averages by applying Simpson's rule, which preserves fourth-order accuracy in space. However, in the case of one dimension, it was shown that the monotonicity of the scheme for discontinuous solutions is better when integral averages are used instead of half-integer values (see [3]).

Since the nondifferentiability of the solution is rather typical of particle transport problems, in this work, we also use an expansion of the set of unknown quantities. In contrast to one dimension, in this case, this set becomes even larger. Specifically, we construct a system of dynamic equations with four unknowns. To derive a high-order bicompact approximation of this equation without splitting in spatial directions or introducing half-integer values, we introduce additional variables, namely, the edge fluxes

$$w^x = \int_{x_l}^{x_{l+1}} u\,dx, \quad w^y = \int_{y_j}^{y_{j+1}} u\,dy \tag{4}$$

and the total flux

$$w = \int_{x_l}^{x_{l+1}} \int_{y_j}^{y_{j+1}} u dy dx. \tag{5}$$

Direct integration of the original equation over a spatial cell gives the following equation for the total flux:

$$\frac{\partial w}{\partial t} + a\left(w^y_{l+1} - w^y_l\right) + b\left(w^x_{j+1} - w^x_j\right) + \sigma w = \int_{y_j}^{y_{j+1}} dy \int_{x_l}^{x_{l+1}} Q(x,y,t)dx. \tag{6}$$

Integrating Eq. (1) with respect to any of the spatial coordinates within a cell, we obtain two relations of the form

$$\frac{\partial w^x}{\partial t} + a(u_{l+1} - u_l) + b\frac{\partial w^x}{\partial y} + \sigma w^x = \int_{x_l}^{x_{l+1}} Q(x,y,t)dx, \tag{7}$$

$$\frac{\partial w^y}{\partial t} + a\frac{\partial w^y}{\partial x} + b(u_{j+1} - u_j) + \sigma w^y = \int_{y_j}^{y_{j+1}} Q(x,y,t)dy. \tag{8}$$

The remaining spatial and time coordinates in these equations are as yet arbitrary. Throughout this paper, we assume that $h_x = x_{l+1} - x_l$ and $h_y = y_{j+1} - y_j$ are local, and the cell index in the mesh sizes is omitted.

To derive an evolution equation for the edge fluxes, the total flux is treated as an iterated integral and the fourth-order accurate Euler–Maclaurin formula (3) is applied to the inner integral:

$$\begin{aligned} w = \int_{x_l}^{x_{l+1}} \int_{y_j}^{y_{j+1}} u dx dy = \int_{y_j}^{y_{j+1}} dy \int_{x_l}^{x_{l+1}} u dx = \int_{y_j}^{y_{j+1}} dy \left(\frac{h_x}{2}\left(u(x_{l+1},y,t) + u(x_l,y,t)\right) - \frac{h_x^2}{12}\left(u'_x(x_{l+1},y,t) - u'_x(x_l,y,t)\right)\right) \\ = \frac{h_x}{2}\left(w^y_{l+1} + w^y_l\right) - \frac{h_x^2}{12}\frac{\partial\left(w^y_{l+1} - w^y_l\right)}{\partial x}. \end{aligned} \tag{9}$$

Replacing the x-derivatives in the last term by those from intermediate relations (8), we obtain

$$\begin{aligned} w = \frac{h_x}{2}\left(w^y_{l+1} + w^y_l\right) - \frac{h_x^2}{12a}\left(-\frac{\partial w^y_{l+1}}{\partial t} - b\left(u_{l+1j+1} - u_{l+1j}\right) - \sigma w^x_{l+1} + \int_{y_j}^{y_{j+1}} Q(x_{l+1},y,t)dy \right. \\ \left. + \frac{\partial w^y_l}{\partial t} + b\left(u_{lj+1} - u_{lj}\right) + \sigma w^x_l - \int_{y_j}^{y_{j+1}} Q(x_l,y,t)dy \right), \end{aligned} \tag{10}$$

which makes it possible to obtain an evolution equation for the edge flux difference w^y:

$$\begin{aligned} \frac{\partial\left(w^y_{l+1} - w^y_l\right)}{\partial t} = \frac{12a}{h_x^2}w - \frac{6a}{h_x}\left(w^y_{l+1} + w^y_l\right) - b\left(u_{l+1,j+1} + u_{l,j} - u_{l+1,j} - u_{l,j+1}\right) \\ - \sigma\left(w^y_{l+1} - w^y_l\right) + \int_{y_j}^{y_{j+1}} \left(Q(x_{l+1},y,t) - Q(x_l,y,t)\right)dy. \end{aligned} \tag{11}$$

Passing from the double integral in (9) to an iterated one in reverse order, in a similar manner, we can obtain an evolution equation for the edge flux difference w^x:

$$\begin{aligned} \frac{\partial\left(w^x_{j+1} - w^x_j\right)}{\partial t} = \frac{12b}{h_y^2}w - \frac{6b}{h_y}\left(w^x_{j+1} + w^x_j\right) - a\left(u_{l+1,j+1} + u_{l,j} - u_{l+1,j} - u_{l,j+1}\right) \\ - \sigma\left(w^x_{j+1} - w^x_j\right) + \int_{x_i}^{x_{i+1}} \left(Q(x,y_{j+1},t) - Q(x,y_j,t)\right)dx. \end{aligned} \tag{12}$$

In this case, the most difficult task is to derive an evolution equation directly for the desired quantities. We introduce the combination

$$\Delta^{xy}(u) = u_{l+1,j+1} + u_{l,j} - u_{l+1,j} - u_{l,j+1}. \tag{13}$$

Since Eqs. (11) and (12) contain this quantity, it is desirable to obtain an evolution equation for it. For this purpose, we consider, for example, the edge flux (the second spatial and time coordinates are arbitrary):

$$\begin{aligned} w^x &= \int_{x_l}^{x_{l+1}} u dx = \left(\frac{h_x}{2}\left(u(x_{l+1}, y, t) + u(x_l, y, t)\right) - \frac{h_x^2}{12}\left(u'_x(x_{l+1}, y, t) - u'_x(x_l, y, t)\right)\right) \\ &= \frac{h_x}{2}\left(u_{l+1} + u_l\right) + \frac{h_x^2}{12a}\left(\left.\frac{\partial u}{\partial t}\right|_{x=x_{l+1}} + b\left.\frac{\partial u}{\partial y}\right|_{x=x_{l+1}} + \sigma u_{l+1} - Q_{l+1} - \left.\frac{\partial u}{\partial t}\right|_{x=x_l} - b\left.\frac{\partial u}{\partial y}\right|_{x=x_l} - \sigma u_l + Q_l\right). \end{aligned} \tag{14}$$

A similar expression can be obtained for w^y.

Then we have

$$\begin{aligned} w^x_{j+1} &= \frac{h_x}{2}\left(u_{l+1,j+1} + u_{l,j+1}\right) \\ &+ \frac{h_x^2}{12a}\left(\frac{\partial u_{l+1,j+1}}{\partial t} + b\frac{\partial u_{l+1,j+1}}{\partial y} + \sigma u_{l+1,j+1} - Q_{l+1,j+1} - \frac{\partial u_{l,j+1}}{\partial t} - b\frac{\partial u_{l,j+1}}{\partial y} - \sigma u_{l,j+1} + Q_{l,j+1}\right). \end{aligned} \tag{15}$$

This relation yields

$$\begin{aligned} \frac{\partial(u_{l+1,j+1} - u_{l,j+1})}{\partial t} &= \frac{12a}{h_x^2} w^x_{j+1} - \frac{6a}{h_x}\left(u_{l+1,j+1} + u_{l,j+1}\right) \\ - b\frac{\partial(u_{l+1,j+1} - u_{l,j+1})}{\partial y} &- \sigma(u_{l+1,j+1} - u_{l,j+1}) + Q_{l+1,j+1} - Q_{l,j+1} \end{aligned} \tag{16}$$

and, with shifted indices,

$$\frac{\partial(u_{l+1,j} - u_{l,j})}{\partial t} = \frac{12a}{h_x^2} w^x_j - \frac{6a}{h_x}\left(u_{l+1,j} + u_{l,j}\right) - b\frac{\partial(u_{l+1,j} - u_{l,j})}{\partial y} - \sigma(u_{l+1,j} - u_{l,j}) + Q_{l+1,j} - Q_{l,j}. \tag{17}$$

Subtracting Eq. (17) from Eq. (16) produces

$$\frac{\partial\Delta^{xy}(u)}{\partial t} = \frac{12a}{h_x^2}\left(w^x_{j+1} - w^x_j\right) - \frac{6a}{h_x}\left(u_{l+1,j+1} + u_{l,j+1} - u_{l+1,j} - u_{l,j}\right) - b\frac{\partial\Delta^{xy}(u)}{\partial y} - \sigma\Delta^{xy}(u) + \Delta^{xy}(Q). \tag{18}$$

As yet, Eq. (18) contains a partial y-derivative. Therefore, it is still unsuitable for deriving a system of four ordinary differential equations (ODEs).

Similar manipulations for w^y yield

$$\frac{\partial\Delta^{xy}(u)}{\partial t} = \frac{12b}{h_y^2}\left(w^y_{l+1} - w^y_l\right) - \frac{6b}{h_y}\left(u_{l+1,j+1} + u_{l+1,j} - u_{l,j+1} - u_{l,j}\right) - a\frac{\partial\Delta^{xy}(u)}{\partial x} - \sigma\Delta^{xy}(u) + \Delta^{xy}(Q). \tag{19}$$

Adding this to the preceding equation, we obtain

$$\begin{aligned} 2\frac{\partial\Delta^{xy}(u)}{\partial t} &= \frac{12a}{h_x^2}\left(w^x_{j+1} - w^x_j\right) - \frac{6a}{h_x}\left(u_{l+1,j+1} + u_{l,j+1} - u_{l+1,j} - u_{l,j}\right) \\ &+ \frac{12b}{h_y^2}\left(w^y_{l+1} - w^y_l\right) - \frac{6b}{h_y}\left(u_{l+1,j+1} + u_{l+1,j} - u_{l,j+1} - u_{l,j}\right) \\ &- a\frac{\partial\Delta^{xy}(u)}{\partial x} - b\frac{\partial\Delta^{xy}(u)}{\partial y} - 2\sigma\Delta^{xy}(u) + 2\Delta^{xy}(Q). \end{aligned} \tag{20}$$

Since the operator Δ^{xy} is only a combination of the indices and signs of the original quantities, its application to the original transport equation (1) gives

$$\frac{\partial\Delta^{xy}(u)}{\partial t}+a\frac{\partial\Delta^{xy}(u)}{\partial x}+b\frac{\partial\Delta^{xy}(u)}{\partial y}+\sigma\Delta^{xy}(u)=\Delta^{xy}(Q),$$

which means that some of the terms in Eq. (20) cancel out; i.e.,

$$\begin{aligned}\frac{\partial\Delta^{xy}(u)}{\partial t}&=\frac{12a}{h_x^2}\left(w^x_{j+1}-w^x_j\right)-\frac{6a}{h_x}\left(u_{l+1,j+1}+u_{l,j+1}-u_{l+1,j}-u_{l,j}\right)\\&+\frac{12b}{h_y^2}\left(w^y_{l+1}-w^y_l\right)-\frac{6b}{h_y}\left(u_{l+1,j+1}+u_{l+1,j}-u_{l,j+1}-u_{l,j}\right)-\sigma\Delta^{xy}(u)+\Delta^{xy}(Q).\end{aligned}\tag{21}$$

This equation determines the evolution of the distribution function.

The system of Eqs. (6), (11), (12), and (21) does not contain spatial derivatives and defines a factorized bicompact scheme of the method of lines for the linear inhomogeneous transport equation in the case of two dimensions. Equation (6) is an exact consequence of the transport equation, while Eqs. (11), (12), and (21) are obtained using formulas that are fourth-order accurate in space. Equation (6) is a classical nonstationary equation, Eqs. (11) and (12) are written for the difference between the desired quantities on neighboring edges, and Eq. (21) is written for combination (13) of node values. System (6), (11), (12), (21) with boundary conditions (2) forms a differential algebraic system. As in the case of one spatial variable, the resulting dynamical system of four equations can be solved using the running calculation method, which is an indirect consequence of the characteristic properties of the transport equation and the compact approximation. The possibility of running computations is confirmed by the structure of the propagation matrix of the resulting system. For the chosen signs of the coefficients $a>0$ and $b>0$, the running computations are directed toward increasing independent variables.

in a similar manner to the one-dimensional case (see [10]), the spectrum of the propagation matrix of system (6), (11), (12), (21) is determined by the 4×4 block matrices on the main diagonal. Assume that the variables to be determined in a given cell are ordered as follows: $\mathbf{v}=\{w,w^y_{l+1},w^x_{j+1},u_{l+1,j+1}\}$, where $n=L(j-1)+l$ determines a generalized index of the current cell. Then we obtain the following dynamical system of the method of lines for the expanded set of variables:

$$\mathbf{v}'_t=\mathbf{A}\mathbf{v}+\mathbf{F},\quad \mathbf{A}=\begin{pmatrix}\mathbf{A}_{11}&0&0&0\\\mathbf{A}_{21}&\mathbf{A}_{22}&0&0\\\cdots&&&\\\mathbf{A}_{N1}&\mathbf{A}_{N2}&&\mathbf{A}_{NN}\end{pmatrix},\tag{22}$$

$$\mathbf{A}_{nn}=\begin{pmatrix}-\sigma&-a&-b&0\\\frac{12a}{h_x^2}&-\sigma-\frac{6a}{h_x}&0&-b\\\frac{12b}{h_y^2}&0&-\sigma-\frac{6b}{h_y}&-a\\0&\frac{12b}{h_y^2}&\frac{12a}{h_x^2}&-\sigma-\frac{6a}{h_x}-\frac{6b}{h_y}\end{pmatrix}.\tag{23}$$

The eigenvalues of the block $\mathbf{A}_{nn}$ determining the behavior of the solution are

$$\lambda_{1,2,3,4}=\left\{-\sigma-\frac{3a}{h_x}-\frac{3b}{h_y}\pm i\sqrt{3}\frac{ah_y\pm bh_x}{h_xh_y}\right\}.\tag{24}$$

3. BICOMPACT TIME APPROXIMATION

Various methods can be used to obtain a time approximation of the resulting system of equations for the expanded set of variables. The methods considered in [1–10] included primarily diagonal implicit Runge–Kutta methods, which have remarkable stability properties. A detailed description of the methods can be found in [24, 25]. They are listed below.

1. **A-stable** third-order accurate Runge–Kutta method with the Butcher tableau

$$\begin{array}{c|c} \mathbf{c} & \mathbf{A} \\ \hline & \mathbf{b}^{\mathrm{T}} \end{array} = \begin{array}{c|ccc} 1/3 & 1/3 & & \\ 1 & 1/3 & 2/3 & \\ 1 & 0 & 0 & 1 \\ \hline & 3/4 & 3/4 & -1/2 \end{array}. \tag{25}$$

2. **L-stable** stiffly accurate third-order accurate Runge–Kutta method with the Butcher tableau

$$\begin{array}{c|c} \mathbf{c} & \mathbf{A} \\ \hline & \mathbf{b}^{\mathrm{T}} \end{array} = \begin{array}{c|ccc} 1/3 & 1/3 & & \\ 1 & 0 & 1 & \\ 1 & 3/4 & -1/12 & 1/3 \\ \hline & 3/4 & -1/12 & 1/3 \end{array}. \tag{26}$$

3. **SDIRK**: singly diagonal implicit stiffly accurate third-order accurate Runge–Kutta method with the Butcher tableau

$$\begin{array}{c|c} \mathbf{c} & \mathbf{A} \\ \hline & \mathbf{b}^{\mathrm{T}} \end{array} = \begin{array}{c|ccc} c_1 & a & & \\ c_2 & a_{21} & a & \\ c_3 & a_{31} & a_{32} & a \\ \hline & b_1 & b_2 & b_3 \end{array}. \tag{27}$$

The coefficients of the stiffly accurate method (including scheme 2) are related as follows:

$$b_1 = a_{31}, \quad b_2 = a_{32}, \quad b_3 = a.$$

The other coefficients of the scheme have the form

$$\begin{gathered} a_{21} = -\frac{a - 1/3}{2(a^2 - 2a + 1/2)}, \\ b_1 = a_{31} = 1 - a - b_2, \quad b_2 = a_{32} = -\frac{2(a^2 - 2a + 1/2)^2}{a - 1/3}, \quad b_3 = a, \end{gathered} \tag{28}$$

where $a = 1 + \sqrt{2}\cos((\varphi + 4\pi)/3)$ and $\varphi = \arccos\left(2\sqrt{2}/3\right)$.

The coefficients c_1, c_2, and c_3 are derived from the unessential Kutta conditions: $c_i = \sum_j a_{ij}$.

This method, like method 2, is L-stable and stiffly accurate.

4. **CROS**: a second-order accurate one-iteration Rosenbrock method with complex coefficients of the form

$$\left(\mathbf{E} - \frac{1+i}{2}\mathbf{A}\tau\right)\mathbf{v} = \frac{1-i}{2}\mathbf{A}\tau\mathbf{w} + \mathbf{F}\left(x, y, t + \frac{\tau}{2}\right), \quad \hat{\mathbf{w}} = \mathrm{Re}(\mathbf{v}). \tag{29}$$

This method (see [26, 27]) is second-order accurate and has the best possible L2-stability and t-monotonicity. In contrast to methods 1–3, it involves one stage but its implementation requires complex arithmetic, which is roughly four times as expensive as real arithmetic. Another shortcoming of the method in the general case is that it involves only one iteration, which imposes a constraint on the time step in the case of strongly nonlinear problems. For the linear transport equation, there is no such constraint.

For all these methods, the portraits of the stability functions in the complete complex plane were presented in [6]. The behavior of the stability functions on the negative real axis is shown in the figure.

Test computations of one-dimensional problems (see [9]) have shown that the results produced by schemes 2 and 3 are fairly close to each other (see the stability function in the figure) and, as predicted by the theory, the error in method 3 is somewhat smaller. For this reason, scheme 2 is not considered in what follows.

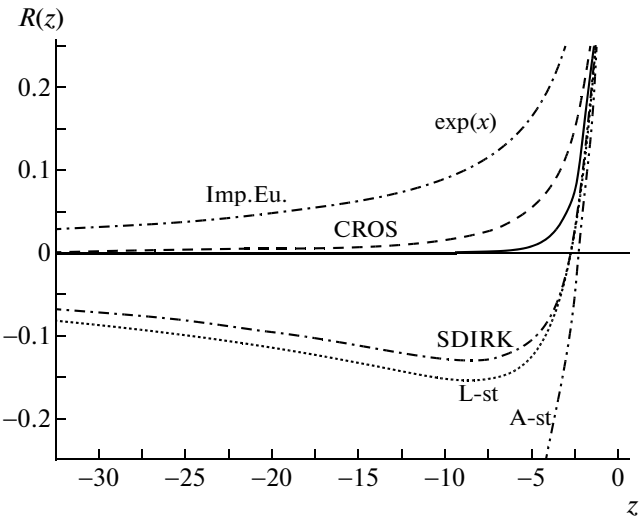

Stability functions of the implicit Runge–Kutta and Rosenbrock methods [27, 28] on the negative real axis for the implicit Euler method (Imp. Eu), A-stable method 1 (A-st), L-stable method 2 (L-st), singly diagonal implicit Runge–Kutta method 3 (SDIRK), and the Rosenbrock scheme with complex coefficients 4 (CROS). For comparison, the figure displays the exponential approximated by all these stability functions.

4. IMPLEMENTATION OF THE BASELINE SCHEME OF FIRST-ORDER ACCURACY IN TIME

For schemes 1 and 2, the baseline scheme is specified by the implicit Euler method. For this reason, we briefly outline its implementation as applied to system (6), (11), (12), (21). Following Samarskii, the variables at a new time level are marked with a cup. Then we have

$$\hat{w} = w - a\tau(\hat{w}^y_{l+1} - \hat{w}^y_l) - b\tau(\hat{w}^x_{j+1} - \hat{w}^x_j) - \sigma\tau\hat{w} + \tau\iint\limits_{\Pi} Q(x,y,\hat{t})dxdy, \tag{30}$$

$$\hat{w}^y_{l+1} = \hat{w}^y_l + w^y_{l+1} - w^y_l + \frac{12a\tau}{h_x^2}\hat{w} - \frac{6a\tau}{h_x}\left(\hat{w}^y_{l+1} + \hat{w}^y_l\right) - b\tau\Delta^{xy}\hat{u} - \sigma\tau\left(\hat{w}^y_{l+1} - \hat{w}^y_l\right) + \tau\int\limits_{y_j}^{y_{j+1}}\left(\hat{Q}_{l+1} - \hat{Q}_l\right)dy, \tag{31}$$

$$\hat{w}^x_{j+1} = \hat{w}^x_j + w^x_{j+1} - w^x_j + \frac{12b\tau}{h_y^2}\hat{w} - \frac{6b\tau}{h_y}\left(\hat{w}^x_{j+1} + \hat{w}^x_j\right) - a\tau\Delta^{xy}\hat{u} - \sigma\tau\left(\hat{w}^x_{j+1} - \hat{w}^x_j\right) + \tau\int\limits_{x_i}^{x_{i+1}}\left(\hat{Q}_{j+1} - \hat{Q}_j\right)dx, \tag{32}$$

$$\begin{aligned}\Delta^{xy}\hat{u} &= \Delta^{xy}u + \frac{12a\tau}{h_x^2}\left(\hat{w}^x_{j+1} - \hat{w}^x_j\right) + \frac{12b\tau}{h_y^2}\left(\hat{w}^y_{l+1} - \hat{w}^y_l\right)\\ &- \frac{6a\tau}{h_x}\left(\Delta^{xy}\hat{u} + 2(\hat{u}_{l,j+1} - \hat{u}_{l,j})\right) - \frac{6b\tau}{h_y}\left(\Delta^{xy}\hat{u} + 2(\hat{u}_{l+1,j} - \hat{u}_{l,j})\right) - \sigma\tau\Delta^{xy}\hat{u} + \tau\Delta^{xy}(\hat{Q}).\end{aligned} \tag{33}$$

Define

$$\delta = 1 + \sigma\tau, \quad \gamma_x = \frac{a\tau}{h_x}, \quad \gamma_y = \frac{b\tau}{h_y}. \tag{34}$$

Then it follows from (30) that

$$\hat{w} = \frac{1}{\delta}\left(w - a\tau(\hat{w}^y_{l+1} - \hat{w}^y_l) - b\tau(\hat{w}^x_{j+1} - \hat{w}^x_j) + \tau\iint\limits_{\Pi} Q(x,y,\hat{t})dxdy\right). \tag{35}$$

Substituting this into (31) and (32) yields a system of two equations for the unknowns $\hat{w}^y_{l+1}$, $\hat{w}^x_{j+1}$:

$$\begin{aligned} a_{11}\hat{w}^y_{l+1} + a_{12}\hat{w}^x_{j+1} &= f_1 - b\tau\Delta^{xy}\hat{u}, \\ a_{21}\hat{w}^y_{l+1} + a_{22}\hat{w}^x_{j+1} &= f_2 - a\tau\Delta^{xy}\hat{u}, \end{aligned} \tag{36}$$

where

$$a_{11} = \delta + 6\gamma_x + 12\frac{\gamma_x^2}{\delta}, \quad a_{12} = 12\gamma_x\gamma_y\frac{h_y}{h_x\delta}, \tag{37}$$

$$a_{21} = 12\gamma_x\gamma_y\frac{h_x}{\delta h_y}, \quad a_{11} = \delta + 6\gamma_y + 12\frac{\gamma_y^2}{\delta}, \tag{38}$$

$$\begin{aligned} f_1 &= w^y_{l+1} - w^y_l + \hat{w}^y_l\left(a_{11} - 12\gamma_x\right) + a_{12}\hat{w}^x_j + \frac{12\gamma_x}{h_x\delta}w \\ &- \sigma\tau(\hat{w}^y_{l+1} - \hat{w}^y_l) + \frac{12\gamma_x^2}{a\delta}\iint\limits_{\Pi}\hat{Q}dxdy + \tau\int\limits_{y_j}^{y_{j+1}}\left(\hat{Q}_{l+1} - \hat{Q}_l\right)dy, \end{aligned} \tag{39}$$

$$\begin{aligned} f_2 &= w^x_{j+1} - w^x_j + \hat{w}^x_j\left(a_{22} - 12\gamma_y\right) + a_{21}\hat{w}^y_l + \frac{12\gamma_y}{h_y\delta}w \\ &- \sigma\tau(\hat{w}^x_{j+1} - \hat{w}^x_j) + \frac{12\gamma_y^2}{b\delta}\iint\limits_{\Pi}\hat{Q}dxdy + \tau\int\limits_{x_l}^{x_{l+1}}\left(\hat{Q}_{j+1} - \hat{Q}_j\right)dx. \end{aligned} \tag{40}$$

System (36) with coefficients (37)–(40) yields relations to the computed coefficients $m^{(k)}$, $n^{(k)}$, $k = 1, 2$, of the form

$$\hat{w}^y_{l+1} = \frac{m^{(1)} + n^{(1)}\Delta^{xy}\hat{u}}{\Delta}, \quad \hat{w}^x_{j+1} = \frac{m^{(2)} + n^{(2)}\Delta^{xy}\hat{u}}{\Delta}, \quad \Delta = a_{11}a_{22} - a_{12}a_{21}. \tag{41}$$

Substituting these relations into (33), we find the following quantity at the new time level:

$$\Delta^{xy}\hat{u} = \frac{\Delta^{xy}u + \frac{12\gamma_x^2}{a}\frac{m^{(2)}}{\Delta} + \frac{12\gamma_y^2}{b}\frac{m^{(1)}}{\Delta} - 12\gamma_x\left[(\hat{u}_{l+1,j} - \hat{u}_{l,j+1}) + \frac{\hat{w}^x_j}{h_x}\right] - 12\gamma_y\left[(\hat{u}_{l,j+1} - \hat{u}_{l+1,j}) + \frac{\hat{w}^y_l}{h_y}\right] + \tau\Delta^{xy}(\hat{Q})}{\delta + 6\gamma_x + 6\gamma_y - \frac{12\gamma_x}{h_x}\frac{n^{(2)}}{\Delta} - \frac{12\gamma_y}{h_y}\frac{n^{(1)}}{\Delta}}. \tag{42}$$

Finally, the sequence of computations is

$$f_1, f_2 \to \Delta, m^{(1)}, n^{(1)}, m^{(2)}, n^{(2)} \to \Delta^{xy}\hat{u} \to \hat{u}_{l+1,j+1} \to \hat{w}^x_{j+1}, \hat{w}^y_{l+1} \to \hat{w}. \tag{43}$$

All the quantities at the new time level in (39)–(42) are known either from the boundary condition or computed in the preceding cell. As a result, running computations can be organized in the method.

The implementation of method 3 (SDIRK) cannot be reduced to a sequence of implicit Euler methods. To implement the Runge–Kutta method for the system of four equations (6), (11), (12), (21), we need to calculate their right-hand sides, which depend on the sought quantities according to Butcher tableau (27). In many respects, this procedure resembles one described above in formulas (30)–(43) for an implicit Euler method, but only for stage right-hand side values. The approach to the elimination of variables in the system of four equations remains the same. We do not overload the presentation with all the computational formulas. For the CROS scheme, the situation is similar.

Remark. System (6)-(11)-(12)-(21) with boundary conditions (2) is a differential algebraic problem. To preserve the order of convergence equal to the order of accuracy, for smooth solutions, a special implementation of the boundary conditions is required in methods 1–3 (see [6]). The order of accuracy can be

Table 1. Error of the schemes in the C norm (left column for each scheme) and the effective convergence order of the schemes (right column) under mesh refinement for Problem 1

$N_x \times N_y \times N_t$	A-stable scheme (1)		Scheme SDIRK (3)		Scheme CROS (4)	
$5 \times 5 \times 3$	2.53709e–3		6.63579e–4		1.79048e–2	
$10 \times 10 \times 6$	3.50538e–4	2.86	9.11253e–5	2.86	5.71823e–3	1.65
$20 \times 20 \times 12$	4.95733e–5	2.82	1.23875e–5	2.88	1.58161e–3	1.85
$40 \times 40 \times 24$	6.05332e–6	3.03	1.62555e–6	2.93	4.14719e–4	1.93
$80 \times 80 \times 48$	7.41003e–7	3.03	2.08211e–7	2.96	1.05814e–4	1.97
$120 \times 120 \times 72$	9.25165e–8	3.00	6.216e–8	2.98	4.72992e–5	1.99

preserved via the transition to a differential problem by replacing boundary conditions (2) with conditions of the form

$$\begin{aligned} u_t(0,y,t) &= p_t(y,t), \quad 0 \le y \le Y, \quad 0 \le t \le T; \\ u_t(x,0,t) &= q_t(x,t), \quad 0 \le x \le X, \quad 0 \le t \le T \end{aligned} \tag{44}$$

and conditions they imply for the time derivatives of edge fluxes, which are implemented using the same Runge–Kutta methods as in the main problem (see [6]).

5. TESTING OF THE METHODS

For this purpose, we used a series of problems with differentiable and piecewise differentiable solutions.

Problem 1. The problem has the infinitely differentiable solution

$$u_{\text{ex}}(x,y,t) = \sin\bigl((x+y-(a+b)t)\bigr).$$

It was solved in the unit cube with the parameters

$$\sigma = 0.3, \quad Q = \sigma u_{\text{ex}}(x,y,t).$$

The initial and boundary conditions were set according to this exact solution, provided that the boundary conditions were properly implemented according to the remark made in Section 4 (see [6]).

Table 1 presents the numerical results produced by solving the problem on meshes of various sizes with parameters $a = 0.1$ and $b = 0.5$.

The experimental order of convergence is close to the theoretically predicted third order, which is determined by the time mesh. The scheme is fourth-order accurate in space. Therefore, the convergence rate is determined, first, by the larger mesh in time and, second, by the lower order of accuracy in time. The third convergence order confirms the validity of the algorithm.

However, a more typical situation in particle transport problems is that the absorption coefficient varies nearly from cell to cell (contact discontinuities, variations in the absorption coefficient due to varying density and temperature in the medium in radiative transfer or neutron transport calculations, etc.). For this reason, we studied another problem, in which the first derivatives of the exact solution are piecewise continuous.

Problem 2. Consider the problem of stationary transport

$$\Omega_x \frac{\partial u}{\partial x} + \Omega_y \frac{\partial u}{\partial y} + \Omega_z \frac{\partial u}{\partial z} + \sigma u = Q \tag{45}$$

in the unit cube. Here, the unit vector $\mathbf{\Omega}$ determines the particle direction. Assume that the absorption coefficient and the source are constant, but there is a central domain where these parameters are specified by different constants. More specifically,

$$\sigma_1 = 1, \quad Q_1 = 0.01$$

everywhere (i.e., in domains 1 + 3 below) except for

$$\text{domain (2):} \begin{cases} 0.25 \le x \le 0.75, \\ 0.25 \le y \le 0.75, \\ 0.25 \le z \le 0.75, \end{cases}$$

in which $\sigma_2 = 0.01$ and $Q_2 = 1$.

Table 2. Error of the schemes in the C norm (left column for each scheme) and the effective convergence order of the schemes (right column) under mesh refinement for Problem 2

$N_x \times N_y \times N_t$	A-stable scheme (1)		Scheme SDIRK (3)		Scheme CROS (4)	
$12 \times 12 \times 8$	2.41762e–1		8.04763e–2		1.75006e–1	
$24 \times 24 \times 16$	2.03971e–1	0.24	4.22492e–2	0.93	1.11359e–1	0.65
$48 \times 48 \times 32$	1.54036e–1	0.40	2.49979e–2	0.76	6.07114e–2	0.87
$96 \times 96 \times 64$	1.20233e–1	0.36	1.58583e–2	0.66	3.86846e–2	0.65

Assume that particles with a distribution function of unit intensity $u_{\text{bound}} = 1$ impinge on the external cube side.

In this case, the exact solution of problem (1), (2) can easily be written out:

$$u(x,y) = e^{-\sigma_1 l_3}\left(e^{-\sigma_2 l_2}\left(e^{-\sigma_1 l_1}u_{\text{bound}} + \frac{Q_1}{\sigma_1}\left(1 - e^{-\sigma_1 l_1}\right)\right) + \frac{Q_2}{\sigma_2}\left(1 - e^{-\sigma_2 l_2}\right)\right) + \frac{Q_1}{\sigma_1}\left(1 - e^{-\sigma_1 l_3}\right), \tag{46}$$

where l_1, l_2, and l_3 are lengths of the characteristic segments in domains 1, 2, and 3. Domains 1 and 3 are defined as follows:

$$\text{domain 1:} \begin{bmatrix} x \le 0.25, \\ y \le 0.25, \\ z \le 0.25, \end{bmatrix}$$

$$\text{domain 3:} \begin{bmatrix} x \ge 0.75, \\ y \ge 0.75, \\ z \ge 0.75, \end{bmatrix} \begin{cases} x \ge 0.25, \\ y \ge 0.25, \\ z \ge 0.25. \end{cases}$$

If a characteristic avoids any of these domains, the corresponding length of the characteristic segment is set equal to zero.

Let z be an analogue of time. If the particle does not move along the z axis ($\Omega_z \neq 0$), elementary rearrangements reduce Eq. (45) to the form of (1):

$$\frac{\partial u}{\partial z} + \frac{\Omega_x}{\Omega_z}\frac{\partial u}{\partial x} + \frac{\Omega_y}{\Omega_z}\frac{\partial u}{\partial y} + \frac{\sigma}{\Omega_z}u = \frac{Q}{\Omega_z}. \tag{47}$$

To this equation, we can apply the solution method proposed above.

Results concerning the grid convergence of the schemes for this problem are presented in Table 2. In this problem, the derivative of the exact solution has a discontinuity on any characteristic passing through the irradiated edges at the entrance to the computational volume and the edges of the internal contact boundary.

For this problem, all the methods exhibit poor convergence, which is caused by the discontinuous first derivatives on the chosen characteristics. In the case of a single spatial variable, where finer meshes can be used, the convergence order of all the methods for a similar problem reached about 0.75. The present result is similar, although further mesh refinement is difficult.

A similar problem in the case of one spatial variable was analyzed in [10]. It was shown that the monotonization method proposed for the homogeneous transport equation (see [7]) is unsuitable for the inhomogeneous transport equation so that a unified monotonization parameter cannot be chosen. A numerical study of the arising errors showed that, according to the stability functions of methods 1–4 (see figure), the three-stage Runge–Kutta methods on characteristics where the solution has a discontinuous derivative lead to large negative values of the unknown function, while the CROS scheme lead to large positive values. Another hybridization method with the use of the CROS scheme was proposed in [10]. In the present work, this approach is extended to two spatial variables.

Recall that the eigenvalues of propagation matrix (22)–(24) are given by

$$\lambda_{1,2,3,4} = \left\{-\sigma - \frac{3a}{h_x} - \frac{3b}{h_y} \pm i\sqrt{3}\frac{ah_y \pm bh_x}{h_x h_y}\right\}.$$

Table 3. Error of the SDIRK scheme in the C norm under mesh refinement for Problem 2 with various absorption coefficients in the central domain

$N_x \times N_y \times N_t$	$\sigma_2 = 5, Q_2 = 5$		$\sigma_2 = 10, Q_2 = 10$		$\sigma_2 = 15, Q_2 = 15$		$\sigma_2 = 20, Q_2 = 20$		$\sigma_2 = 50, Q_2 = 50$	
$12 \times 12 \times 8$	8.92568e–2		1.52769e–1		2.04226e–1		2.4261e–1		3.67529e–1	
$24 \times 24 \times 16$	4.96752e–2	0.85	8.78582e–2	0.80	1.22223e–1	0.74	1.52449e–1	0.67	2.69412e–1	0.45
$48 \times 48 \times 32$	2.55867e–2	0.96	4.52929e–2	0.96	6.43904e–2	0.92	8.27451e–2	0.88	1.71823e–1	0.65
$96 \times 96 \times 64$	1.71114e–2	0.58	2.95695e–2	0.62	4.07905e–2	0.66	5.07001e–2	0.71	9.69258e–2	0.83

Table 4. Error of the CROS scheme in the C norm under mesh refinement for Problem 2 with various absorption coefficients in the central domain

$N_x \times N_y \times N_t$	$\sigma_2 = 5, Q_2 = 5$		$\sigma_2 = 10, Q_2 = 10$		$\sigma_2 = 15, Q_2 = 15$		$\sigma_2 = 20, Q_2 = 20$		$\sigma_2 = 50, Q_2 = 50$	
$12 \times 12 \times 8$	8.93476e–2		1.51749e–1		2.02113e–1		2.43838e–1		3.58145e–1	
$24 \times 24 \times 16$	5.14501e–2	0.80	8.55311e–2	0.83	1.17070e–1	0.79	1.45001e–1	0.75	2.66779e–1	0.42
$48 \times 48 \times 32$	2.53810e–2	1.00	6.11941e–2	0.48	7.22182e–2	0.70	9.35314e–2	0.63	1.69586e–1	0.65
$96 \times 96 \times 64$	1.911373e–2	0.41	3.46103e–2	0.82	5.11098e–2	0.50	7.55688e–2	0.31	1.12186e–1	0.60

Table 5. Error in the monotonized SDIRK scheme with the use of CROS (48), (49) in the C norm under mesh refinement for Problem 2 with various absorption coefficients in the central domain at use of

$N_x \times N_y \times N_t$	$\sigma_2 = 5, Q_2 = 5$		$\sigma_2 = 10, Q_2 = 10$		$\sigma_2 = 15, Q_2 = 15$		$\sigma_2 = 20, Q_2 = 20$		$\sigma_2 = 50, Q_2 = 50$	
$12 \times 12 \times 8$	8.94596e–2		1.51980e–1		2.00897e–1		2.35083e–1		7.02316e–1	
$24 \times 24 \times 16$	4.97399e–2	0.85	8.78268e–2	0.79	1.22049e–1	0.72	1.51898e–1	0.63	3.81052e–1	0.88
$48 \times 48 \times 32$	2.55867e–2	0.96	4.52931e–2	0.96	6.43833e–2	0.92	8.27194e–2	0.94	1.70701e–1	1.16
$96 \times 96 \times 64$	1.71115e–2	0.58	2.95695e–2	0.62	4.07905e–2	0.66	5.07001e–2	0.71	9.6865e–2	0.82

In the case of large optical depths, for the computation of a given cell, the principal part of all the eigenvalues is $z = -\sigma_{l,j}\tau$. When the stationary equation (45) is transformed into (47), this part becomes

$$z = -\sigma_{l,j}h_z/\Omega_z \approx \lambda h_z.$$

Then, for each cell, r can be determined by the condition

$$rR_{\mathrm{CROS}}(z) + (1-r)R_{\mathrm{SDIRK}}(z) = \exp(z), \quad z = -\sigma_{l,j}h_z/\Omega_z, \tag{48}$$

or

$$r = \frac{\exp(z) - R_{\mathrm{SDIRK}}}{R_{\mathrm{CROS}} - R_{\mathrm{SDIRK}}}.$$

Finally, after computing the given cell, the solution is monotonized using the formula

$$\hat{u}_{l+1,j+1} = r\hat{u}_{l+1,j+1(\mathrm{CROS})} + (1-r)\hat{u}_{l+1,j+1(\mathrm{SDIRK})}. \tag{49}$$

This linear monotonizing procedure ensures at least second-order accuracy, since $r = O(z)$, $z \to 0$.

Table 3 presents the numerical results obtained for Problem 2 by applying the proposed monotonization for various optical depths of the central domain. The parameters were specified as

$$\Omega_x = 0.5\sqrt{(1-\Omega^2{}_z)}, \quad \Omega_y = \sqrt{(1-\Omega^2{}_z)}\sqrt{(1-0.5^2)}, \quad \Omega_z = 0.9.$$

For optically thick media, the limiting value in the central domain is given by Q_2/σ_2. For most of the considered problems, this ratio is equal to unity. As the optical depth increases, the absolute error in all the methods increases as well, which is especially critical for the largest optical depth. An unpleasant feature of the SDIRK method is that it produces unphysical negative solutions.

Problem 3. Consider a hybrid of problems 1 and 2: suppose that the solution is infinitely differentiable, but the absorption coefficient is piecewise constant as in Problem 2. The differentiability of the solu-

Table 6. Error of the schemes in the C norm under mesh refinement for Problem 3 with various absorption coefficients in the central domain

$N_x \times N_y \times N_t$	A-stable scheme (1)		Scheme SDIRK (3)		Scheme CROS (4)	
$12 \times 12 \times 8$	8.713e–3		3.48489e–3		1.12264e–1	
$24 \times 24 \times 16$	2.3283e–3	1.90	7.93494e–4	2.13	3.16652e–2	1.90
$48 \times 48 \times 32$	6.138e–4	1.92	2.05673e–4	1.95	8.49690e–3	1.90
$96 \times 96 \times 64$	1.5756e–4	1.96	5.24071e–5	1.97	2.20383e–3	1.95

tion is ensured by the right-hand side of the transport equation: $\sigma_1 = 1$, $\sigma_2 = 0.01$, $u_{ex}(x,y,t) = \sin\big((x + y - (a + b)t)\big)$, $Q = \sigma u_{ex}(x,y,t)$. The convergence results for this method are given in Table 6.

As can be seen, the methods have the second limiting order of convergence in this problem. An increase in this characteristic on coarse grids is associated with the fourth order of accuracy in space. Possibly, the decrease in the convergence order of the Runge–Kutta methods down to the second in the case of a discontinuous absorption coefficient is caused by the transmission of stage data between cells with different absorption coefficients. In a sense, this situation is similar to that arising when the boundary condition is specified by the exact solution without reducing the differential algebraic problem to differential one (44) (see [6]).

6. SUMMARY AND CONCLUSIONS

A method for solving a linear inhomogeneous transport equation was proposed that is fourth-order accurate in space and third-order accurate in time. The method does not innvolve splitting in directions or introducing additional values of the unknown function at half-integer nodes. A bicompact scheme was constructed using the method of lines for an expanded set of variables. In comparison with the one-dimensional case, the number of desired quantities was twice as large. The scheme is a running calculation one, since the propagation matrix can be inverted using only variables specified in the current cell.

In the case of the three-dimensional stationary transport equation, the time derivative can be replaced by the third spatial derivative.

For an infinitely differentiable solution, the order of convergence coincides with the order of accuracy when the boundary conditions are suitably approximated and the absorption coefficient is a constant. When the absorption coefficient varies from cell to cell, the actual order of convergence is reduced to the second even for an infinitely differentiable solution. For a piecewise differentiable solution, the convergence order is even lower and is difficult to determine even experimentally.

Proposed in [10] for solving the inhomogeneous transport equation, the monotonizing procedure based on a one-iteration single-stage Rosenbrock scheme with complex coefficients (CROS) was also successfully applied inities this case. As a result, the error of the method based on a third-order accurate singly diagonal implicit Runge–Kutta method (SDIRK) was reduced considerably.

In the case of three dimensions, it can be expected that the number of desired quantities would increase twice (to eight), which would lead to increased difficulties in resolving the propagation matrix within a cell.

ACKNOWLEDGMENTS

This work was supported by the Russian Foundation for Basic Research (project no. 11-01-00389a) and by a grant from the Government of the Russian Federation in the framework of resolution no. 220 “On measures to attract leading scientists to Russian higher educational institutions” under contract no. 11.G34.31.0072 between the Ministry of Education and Science of the Russian Federation, Leading Scientist, and the Moscow Institute of Physics and Technology (State University).

REFERENCES

1. B. V. Rogov and M. N. Mikhailovskaya, “Fourth-order accurate bicompact schemes for hyperbolic equations,” Dokl. Math. **81**, 146–150 (2010).
2. B. V. Rogov and M. N. Mikhailovskaya, “Monotone bicompact scheme for a linear advection equation,” Mat. Model. **23** (6), 98–110 (2011).

3. B. V. Rogov and M. N. Mikhailovskaya, "Monotone bicompact schemes for a linear advection equation," Dokl. Math. **83**, 121–125 (2011).
4. B. V. Rogov and M. N. Mikhailovskaya, "Monotone high-order accurate compact scheme for quasilinear hyperbolic equations," Dokl. Math. **84**, 747–752 (2011).
5. M. N. Mikhailovskaya and B. V. Rogov, "Bicompact monotone schemes for the multidimensional linear advection equation," Mat. Model. **23** (10), 107–116 (2011).
6. E. N. Aristova and B. V. Rogov, "Implementation of boundary conditions in bicompact schemes for a linear advection equation," Mat. Model. **24** (10), 3–14 (2012).
7. M. N. Mikhailovskaya and B. V. Rogov, "Monotone compact running schemes for systems of hyperbolic equations," Comput. Math. Math. Phys. **52**, 578–600 (2012).
8. B. V. Rogov, "High-order accurate monotone compact running scheme for multidimensional hyperbolic equations," Comput. Math. Math. Phys. **53**, 205–214 (2013).
9. E. N. Aristova, D. F. Baidin, and B. V. Rogov, "Bicompact schemes for an inhomogeneous linear advection equation," Mat. Model. **25** (5), 55–66 (2013).
10. E. N. Aristova, "Bicompact schemes for the inhomogeneous linear advection equation in the case of large optical depths," Mat. Model. **25** (10), (2013).
11. A. V. Shil'kov, Preprint No. 100, IPM AN SSSR (Institute of Applied Mathematics, USSR Academy of Sciences, Moscow, 1987).
12. A. V. Shil'kov, Preprint No. 125, IPM AN SSSR (Institute of Applied Mathematics, USSR Academy of Sciences, Moscow, 1988).
13. I. L. Tsvetkova and A. V. Shil'kov, "Averaging of transport equation in a resonantly absorbing medium," Mat. Model. **1** (1), 91–100 (1989).
14. I. L. Tsvetkova and A. V. Shil'kov, Preprint No. 100, IPM AN SSSR (Institute of Applied Mathematics, USSR Academy of Sciences, Moscow, 1989).
15. A. V. Shil'kov, "Averaging of cross sections and spectrum in neutron transport," Mat. Model. **3** (2), 63–81 (1991).
16. A. V. Shilkov, "Averaging of cross-sections and energy spectrum in neutron transport problems," *Proceedings of the International Topical Meeting on Advances in Mathematics, Computations, and Reactor Physics* (Pittsburgh, USA, 1991), Vol. 3, 13.1.1.
17. S. V. Mozheiko, I. L. Tsvetkova, and A. V. Shil'kov, "Calculation of radiative transfer in a hot air," Mat. Model. **4** (1), 65–82 (1992).
18. A. V. Shil'kov, I. L. Tsvetkova, and S. V. Shil'kova, "ATRAD code system and data base for precise calculations of atmospheric radiation," Mat. Model. **6** (7), 91–102 (1994).
19. A. V. Shilkov, "Generalized multigroup approximation and Lebesgue averaging method in particle transport problems," Transp. Theory Stat. Phys. **23**, 781–814 (1994).
20. A. V. Shil'kov, I. L. Tsvetkova, and S. V. Shil'kova, "ATRAD System for atmospheric radiation computation: Lebesgue averaging of radiation spectra and absorbing cross sections," Mat. Model. **9** (6), 3–24 (1997).
21. A. V. Shil'kov, S. V. Shil'kova, V. Ya. Gol'din, and E. N. Aristova, "Efficient precise computations of atmospheric radiation based on the ATRAD system," Dokl. Math. **60**, 469–471 (1999).
22. A. V. Shil'kov, S. V. Shil'kova, V. Ya. Gol'din, and E. N. Aristova, "ATRAD system for atmospheric radiation computation: Solar radiation transfer in the midlatitude summer atmosphere," Mat. Model. **11** (5), 117–125 (1999).
23. A. V. Shil'kov, M. N. Gertsev, E. N. Aristova, and S. V. Shil'kova, "Method of line-by-line reference computation of atmospheric radiation," Komp'yut. Issled. Model. **4**, 553–562 (2012).
24. K. Dekker and J. G. Verwer, *Stability of Runge–Kutta Methods for Stiff Nonlinear Differential Equations* (North-Holland, Amsterdam, 1984).
25. E. Hairer and G. Wanner, *Solving Ordinary Differential Equations II: Stiff and Differential-Algebraic Problems* (Springer-Verlag, Berlin, 1996).
26. H. Rosenbrock, "Some general implicit processes for numerical solution of differential equations," Comput. J. **5**, 329–330 (1963).
27. N. N. Kalitkin, "Semi-implicit schemes for highly stiff problems," in *Encyclopedia of Low-Temperature Plasmas* (Yanus-K, Moscow, 2008), Vol. VII-1, Part 1, pp. 153–171 [in Russian].

Translated by I. Ruzanova